Eur. Phys. J. B **43**, 549–555 (2005)
DOI: 10.1140/epjb/e2005-00089-3

THE EUROPEAN PHYSICAL JOURNAL B

A quantum mechanically study of silicon nanograins with an aluminum overlayer: structural properties and electronic charge

A.M. Mazzone[a]

CNR-IMM, Sezione di Bologna, Via Gobetti 101, 40129 Bologna, Italy

Received 4 February 2004 / Received in final form 1st December 2004
Published online 30 March 2005 –

Abstract. The purpose of this study is the evaluation of the effects of a metallic overlayer on nanocrystalline silicon grains and is based on the Hartree-Fock formulation at semiempirical level and on the Density Functional theory. The structures considered are crystalline grains with a spherical, columnar or T-shaped structure. The ones with mixed composition are constructed by depositing an aluminum layer on the grains with the plated form. The calculations indicate that the aluminum atoms retain the layered distribution without clustering, which is also a property of the bulk samples. The evaluation of the Fermi level suggests the formation of a Schottky barrier and the features of the states localized at the interface indicates quantum confinement. Both properties would be of interest for electronic devices at the nanoscale. However the strength of bonding is generally lower in the structures with contacts and this casts doubts on the stability of structures of this mixed type.

PACS. 71.15.Mb Density functional theory, local density approximation, gradient and other corrections – 81.10.Aj Theory and models of crystal growth; physics of crystal growth, crystal morphology and orientation

1 Introduction

In the last several years there has been a large growth of research efforts in nanotechnology and the development of electronic devices at the nanoscale, in particular, has attracted considerable attention. The studies in this field have demonstrated that the interactions of the active region of the device with the electrodes play a critical role on the transport properties of the entire device. However the prediction of these effects is difficult and the number of studies in this area is still limited. A general formulation of transport in quantum structures was first presented in [1] and successive elaborations focused on nanowires and organic molecules. Covalent systems were considered in [2–4]. These works deal with carbon nanotubes and are based on standard total energy calculations, such as Density Functional and Hartree-Fock theories. However in [3,4] a direct evaluation at *ab initio* level of the current-voltage characteristics is presented whereas [2] is limited the structural and electronic properties of the carbon atoms interacting with the metallic ones.

Owing to the widespread use of nanocrystalline silicon for the fabrication of electronic, opto-electronic and photovoltaic devices, this study deals with silicon grains coated with metallic layers. These structures can be regarded as electronic devices with an atomic scale. The focus of the calculations, as in [2], is on their structural properties and on their electronic charge. The approach is based on both the semiempirical Hartree-Fock and the Density Functional formulation and complements, using higher level calculations, a similar study on different silicon systems, i.e. surface steps and large clusters ([5]. An abridged version of the present paper, with different aims and finalities, has been presented in [6]). The results describe structural and electronic properties of grains whose shape and size is absent from the current literature and offer suggestions on plausible features of their current-voltage characteristics.

2 Computational details

Standard practice indicates that nanocrystalline silicon is formed by crystalline grains separated by amorphous regions. The grain shape is amenable to two simple forms, i.e. spherical or columnar, with a linear dimension in a range from a few to some hundreds nm [7–9]. Twin defects are normally present and play an important role in the growth of the nanocrystals [9]. The state-of-the art in calculations witnesses the complexity of the study of these structures. Accurate *ab initio* evaluations are available for

[a] e-mail: mazzone@bo.imm.cnr.it

small-medium size clusters with a size N in the range 40 atoms. The number of studies, however, substantially shrinks with the increase of N. For $N \geq 100$ the focus of the calculations is on effects of quantum confinement. This limits the choice of the cluster geometry and spherical models are almost universally adopted (see [10–14] and references therein).

The structures considered in this work extend the study of the large size beyond the spherical shape so far considered. In particular, attention is paid to large-angle boundaries which are difficult to model even in a continuum approach. Accordingly, the geometries fall into three groups, i.e. spherical, columnar and geminate. The spherical and the columnar models, which represent the spongy and the columnar grains, are obtained by carving a sphere into a cubic crystal or by cutting it parallel to the (100) planes. The section of the columnar structure is squared. The linear dimension of the grain section and its length L vary between 5–10 and 5–40 Å, respectively. Grains with the longest L, owing to their filamentary shape, have to be regarded as nanowires. The geminate structures account for twinned configurations arising from coalescence during growth and offer a practical example of structures with large-angle boundaries. These grains are formed by two adjoined columnar grains perpendicular to each other. The ratio between the length of the two parts varies between 1/4 and 1/2 for the larger and the smaller grains, respectively. With this dimensioning grains of similar size are produced in the three groups and the number of atoms, N, falls homogeneously in the range 30–270 atoms. Therefore the larger grains are comparable with the smaller ones observed in experiments (below columnar, spherical and geminate structures are indicated as 'C', 'S' and 'T-shaped' or 'T', respectively. A sketchy plot of the three structures is presented in Fig. 1).

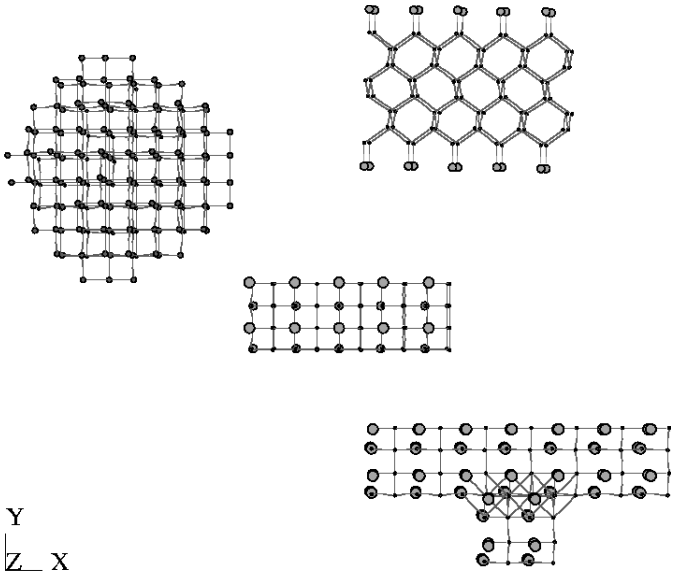

Fig. 1. Spherical, columnar and T-shape grains (from top to bottom). Plane view of the unrelaxed lattice.A lateral view of the columnar structures along (110) is on the right (top). Columnar and T-shaped grains contain silicon and aluminum atoms, marked by the small and large circles, respectively. The size of the circles showing silicon locations decreases going towards the grain interior. Nearest neighbour bonds among silicon and aluminum atoms are traced to give a visual guidance. The lateral displacement of the aluminum atoms (see text) is enhanced in the figure to avoid overlapping with the silicon underneath.

Owing to its many applications in silicon technology and to its simple electronic structure, aluminum represents the metal of choice for studies with quantum mechanical detail and has been adopted for the following calculations. The Si/Al systems consist on columnar structures (i.e. C or T grains) sandwiched between two aluminum films (as shown by Fig. 1. Further details on the locations of the aluminum atoms are reported in Sect. 4). The plated form of these grains, in fact, avoids the irregular decoration observed for spherical structures (for adsorption on spherical clusters see for instance [15]). To offer a comparative insight on the effects of boundaries atoms also a limited number of calculations on grains with hydrogen terminations has been performed. These structures contain a number of H atoms approximately equal to the one of the Al atoms in Si/Al grains of equal size. The H atoms lie on the grain boundaries in a tetrahedral position at a distance 1.5 Å from the nearest silicon atom.

For the evaluation of the structural and electronic properties of the systems defined above two well-grounded Hamiltonians, i.e. semiempirical Hartree-Fock and Density Functional Theory (indicated below as SE and DFT, respectively), have been adopted. The obvious advantage of SE is a limited requirement of computer times, which for large structures scales from several days to several hours. However the parametrization is generally constructed out a large database of molecules and atoms. Its validity is dubious for structures of large size which represent a case significantly different from the reference ones. On the other side, in DFT many important quantities, such as exchange-correlation functionals and pseudopotentials, have a semiempirical ground and the basis set is by necessity incomplete. The comparison of the two methods allows a clear identification of the effects of these uncertain inputs.

The semiempirical Hamiltonian, known by the acronym of AM1 in the chemical literature, belongs to the Modified Neglect of Diatomic Overlap (MNDO) method in the restricted Hartree-Fock formulation (the software is taken from the MOPAC suite of programs [16]). In AM1 only valence electrons are treated explicitly by the use of s and p orbitals. The overlapping and coulomb integrals, needed by the Hartree-Fock formulation, are treated at MNDO level neglecting three-centers interactions and fitting their multipole expansion to the heat of formation, electron affinity and vibrations of atoms and molecules. Literature results indicate that AM1 successfully describes large silicon systems, like silicon surfaces and silloxenix materials (an extensive bibliography on this subject can be found [6,17]). For DFT calculations the SIESTA code [19] has been adopted. In these calculations an extensive testing has been performed on the potentials and basis sets

using both the LDA Perdew-Zunger and the GGC Perdew-Burke-Enrzerhof functionals and single- or double-ζ basis sets. These results will be briefly illustrated in the last section. Unless otherwise specified, the simulation conditions are: LDA, double-ζ plus polarization basis sets, the Troullier-Martins pseudo-potentials and a grid cutoff equal to 100 Ry. In both SE and DFT calculations the most probable grain shape is constructed by relaxing the structure to an energy minimum.

Owing to the size and complexity of the structures examined in this study, several parameters are needed for their characterization. They can be distinguished into structural and electronic and their list is as follows. The structural parameters are the grain volume *Vol*, the number of boundary atoms, the coordination and the spread Z of the height of the aluminum atoms. *Vol* is measured from the parallelepiped which envelops the grain and boundary atoms are the ones at a distance less than a_o ($a_o \sim 1.92$ Å) from the boundary planes of the parallelepiped. The coordination is the average number of atoms within a distance approximately equal to 2.3 Å from a given atom. For Al the coordination radius has been increased to ∼5 Å, owing to the large initial distance among these atoms (see below). Z is the average of the coordinates of the aluminum atoms along the direction z orthogonal to the initial deposition plane. The quantities used to define the electronic charge are the Fermi and binding energy, E_f and E_b, the Density of States (DOS. In DOS plots the energy reference is on E_f) and the ionization potential I_p (the I_p value is the HOMO level in the eigenvalues spectrum). Only SE, which uses direct space, has been adopted for the I_p evaluation. In SIESTA this calculation is performed in momentum space. It requires a large number of bands and, as reported in [25], is extremely sensitive to the solution method adopted for the Hamiltonian and has therefore been discarded. In previous works [5] also the Mulliken charge has been used together with the other electronic parameters. However the comparison between DFT and SE indicated that this evaluation, owing to the minute amount of the exchanged charge, is critical and leads to contradictory results. In the present study the Mulliken charge has been omitted. In the following plots missing points indicate that the accuracy of their evaluation is insufficient.

3 Properties of the silicon nanograins

This section describes the properties of silicon grains in absence of the metallic overlayer. To set the stage briefly, we recall some experimental and theoretical data on silicon clusters. The shape of the clusters with a size N in the range 10 is now well assessed [20–22]. At $N \geq 4$ the clusters acquire a three-dimensional shape and grow by the accretion of capping terminations placed at the corners or at the centers of the faces (see [23–26] and the bibliography therein reported). Up to $N \leq 60$ the polymorphism, typical of the bulk state of silicon, leads to an explosive growth of the number of possible structures. Generally, these clusters have an amorphous core and cage-like units

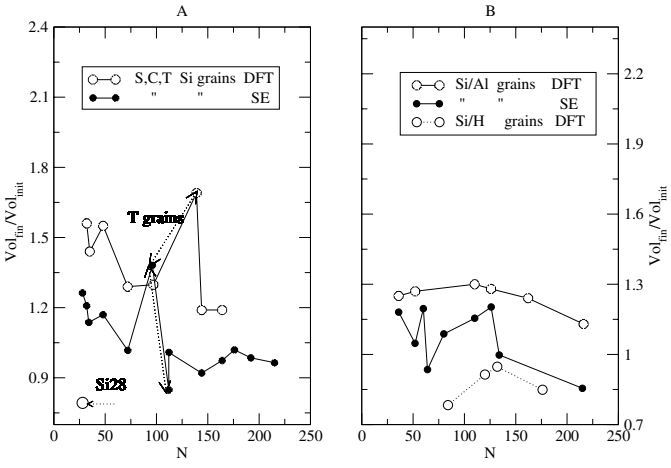

Fig. 2. Structural parameters in the optimized grains. The volume change Vol_{fin}/Vol_{init} in Si (DFT and SE), in Si/Al (DFT and SE) and Si/H (DFT) (Figs. 2A and B, respectively). Data points of the T-grains, showing a large oscillation of Vol_{fin}/Vol_{init}, have been marked by a dotted line and by arrows. Also the spherical cluster Si28 has been marked by an arrow.

may exist on the cluster boundaries. For $N \geq 100$ only the spherical shape has been considered. These clusters retain, in essence, the crystalline lattice of the bulk samples [7], though the size required for the installment of bulk properties is debated. Literature results indicate that this quantity critically depends on the calculation method and values of 50 and 4000 atoms have been reported [11]. Furthermore the surface of large spherical grains reconstructs when the curvature exceeds a critical limit and atoms on close planes rearrange towards the formation of a continuum. The presence of passivating hydrogen atoms leads to a grain surface containing dimerized silicon atoms and mono-, di-hydrided groups reminiscent of the ones observed on H-covered silicon surfaces [11,12,14].

These findings suggest that the grains considered in this study have a crystalline lattice, at least at the larger size. However the grains contain also several anomalous bonding configurations, i.e. step-edge atoms in the spherical grains, corner atoms in the columnar and T-shaped ones and multiply-coordinated atoms at the junctions between the two columnar grains in T (these bonds are marked by the lines in Fig. 1). This suggests that lattice reconstruction is important and has profound effects on the grain shape.

The structural properties and the properties of the electronic charges of the silicon nanograins are illustrated in Figures 2, 3 and 4, 5, respectively. The quantity reported in Figure 2 is the ratio Vol_{fin}/Vol_{init} between the value of the grain volume at the end and at the beginning of the energy minimization and the plot collects all the results obtained for the three structural groups. The change of the grain volume (Fig. 2A) is modest, especially at the larger size. The volume increase, observed at small N, suggests the formation of long bonds, which is typical of the amorphous phase of silicon (the density of amorphous and

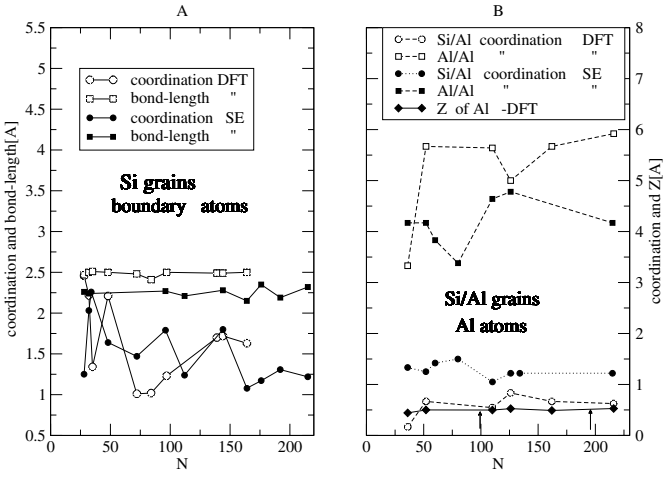

Fig. 3. Structural parameters of the optimized grains. The coordination and bond-length of boundary atoms in silicon grains (A), the coordination, bond-length and height Z of aluminum atoms (B). The plots use the same vertical axis for coordination, bond-length and Z. The unit for lengths is Å.

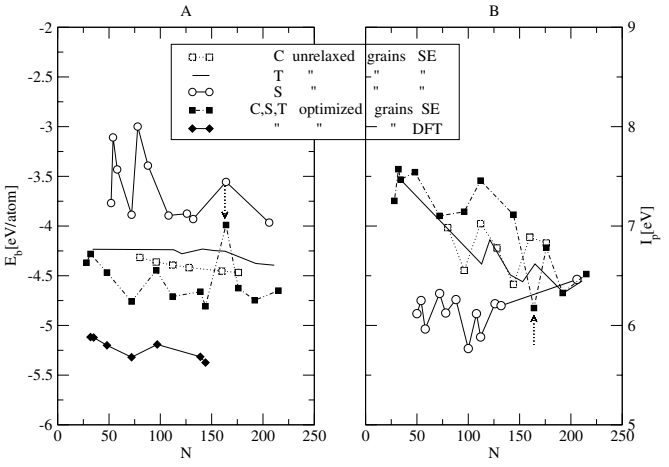

Fig. 4. The functional dependence of E_b (panel A) and I_p (panel B) on the grain size and shape for the pure silicon grains.

crystalline silicon is 2.29 and 2.33 g/cm^3, respectively). In agreement with a partially amorphous structure, the coordination of the boundary atoms (Fig. 3A) is low and fluctuates around the value 2, which is also the coordination of the surface atoms with their back-bonds in the unreconstructed Si(100) (the bondlengths of these surface atoms are 2.5 and 2.9 Å, respectively). The largest values of Vol_{fin}/Vol_{init} and the largest oscillations of this parameter have been found in the T-family (the data-points belonging to this family and showing the above property are marked by the arrows and the lettering 'T grains' in the figure). In the T group a large volume expansion arises from the relaxation of the corner atoms whose number is almost double than in the columnar grains while the volume contraction is attributable to the cohesion of the multiply coordinated atoms at the junction between the two grains (the bonds among those atoms are visible in Fig. 1). However a large Vol_{fin}/Vol_{init} is also observed

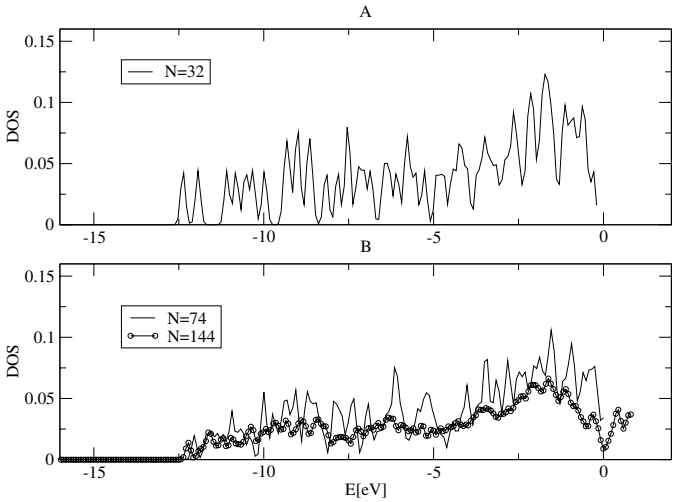

Fig. 5. The DOS plot in Si grains projected on the average atom. The plot shows the N dependence of this parameter.

for the spherical grain of size $N = 28$ (this value, marked by the arrow in Fig. 2A, is outside the line used for the others) which has a large inward relaxation. This feature is in agreement with the puckered shape predicted for clusters of this size in [14]. Generally, the volume change produces atomic displacements with a random direction and with an amplitude in the range 0.1–0.5 Å. This leads to irregular shapes whose gross form is still reminiscent of the initial one. Owing to this irregular character, the presentation of the relaxed grain lattices is of little physical significance and has been omitted. In the context of this study the important results of these calculations is that the grain surface has a corrugated structure with weakly bonded atoms.

The plots in Figure 4 describe the functional dependence of E_b and I_p on the grain size and shape. In order to render more transparent the effects arising from the energy optimization either a relaxed or a rigid lattice model has been applied in SE calculations. In all cases the values of E_b and I_p are reminiscent of the cohesive energy of the bulk silicon and of the ionization potential of the silicon atom (it is known that the bulk cohesive energy has the same physical meaning of E_b and the reverse sign. For crystalline silicon the experimental value of this energy is 4.63 eV and the ionization potential of the silicon atom is 8.15 eV. The DFT evaluation of the bulk cohesive energy is in the range 5.6 eV [19,20]). In the grains, however, the value of E_b increases, as clearly seen in DFT calculations, and the one of I_p decreases with respect to these reference values and both quantities have a fluctuating dependence on N. These properties indicate a weaker bonding than in the bulk and are not uncommon in the literature on the silicon clusters. In fact an oscillatory behaviour of the HOMO level is reported in [25] for silicon clusters with $N \leq 20$ and, as for I_p, the amplitude of these oscillations is around 1 eV. Furthermore the properties of E_b and I_p depend on the details of the grain structure. In fact, the comparison between the unrelaxed lattices and the optimized ones shows that the oscillations are more prominent in the former case, though in the spherical grains the

optimized structures may retain properties peculiarly close to the ones in the unrelaxed lattice (as shown by the examples marked by the arrow in Figs. 4A and 4B).

Subtle effects of the size are shown by the density of states (Fig. 5). It is generally accepted that for nanostructures the DOS shape is indicative of quantum confinement. For linear systems this appears in an E^n behaviour with $n \sim 1/2$ and in the formation of van Hove singularities. However also quasi-particle states leading to separate linewidths in the DOS plot have been attributed to the same quantum origin [28]. The DOS plot of Si nanograins shows a structured shape composed by minibands at small N (Fig. 5A) which changes into a unique broadband, featureless curve at large N (Fig. 5B). No clear dependence on the grain structure has been found for these features. The formation of minibands is attributed to charge exchanges and hybridization of the quasi-particle states of the isolated atoms. A similar shape, with a similar bandwidth and somewhat larger gaps, is reported in [25] for $N = 19$. On the other side, the broadband structure (Fig. 5B) is typical of solids and in the field of clusters occurs for large, three-dimensional structures. A similar band shape has been also reported in [26] for silicon clusters of size $N = 28$. The divergences between [25,26] and our results have only a qualitative meaning and are attributable to the different shapes of the clusters considered in this study with respect to ones considered in [25,26].

4 The nanograins with the aluminum coating

Metal-semiconductor interfaces are important because Schottky barriers, a major component of solid-state devices, are formed by such interfaces. Therefore a large number of experimental and theoretical investigations have been devoted to their study. In particular, the adsorption of Al on Si(111) has been studied experimentally with many surface techniques and theoretically by the self-consistent pseudo-potential technique, extended Hückel theory and by Hartree-Fock [27,29–32]. These studies have shown several possible adsorption sites and a strong bonding between the adsorbate and the adsorbing medium. Known adsorption sites are substitutional, atop, open and eclipsed with a binding strength in the range of a few eV. In both SE and DFT calculations the atop location (i.e. with the aluminum atom on top of a silicon atom at a distance $\sim$2 Å above it and slightly horizontally displaced) was chosen as the starting configuration for lattice optimization. The aluminum coverage has been chosen so that the average Al/Al distance, i.e. 3.83 Å, is equal to the Si-Si distance on the unreconstructed Si(100).

In the context of this study important questions are if the aluminum atoms maintain the initial layered shape without clustering and intermixing and how the intrinsic properties of the grains are altered by the the presence of the overlayer. A comparison between the structural properties of the Si/Al and Si systems is presented in Figures 2 and 3. These data indicate that the Si/Al structures retain, in essence, the properties of the Si ones and the lattice views of the Si/Al grains show that the volume change has the same mode of relaxation described in the previous section for Si grains. Both features are justified by the low Al content in the compound grains (the Al fraction is generally $\leq$0.3 of the total number of atoms). However several details are worth being underlined. First, turning to the comparison with H, it is known that hydrogenation has only a passivating action on dangling silicon orbitals. In agreement with this property, in our calculations the volume of the Si/H grains tends to shrink (Fig. 2B), which indicates the formation of the short bonds typical of the silicon surfaces. The plots in Figures 2A, 2B show that the ratio Vol_{fin}/Vol_{init} in Si/Al has a value intermediate between the one in Si and in Si/H and this indicates that the quality of the Si/Al bonds is similar to the quality of the Si/H ones. In fact, the low valence of the Al atom as well as the low cohesive energy of crystalline Al in comparison with Si (the experimental value of the cohesive energy of *f.c.c.* Al is 3.39 eV) suggests the formation of electron-deficient, and therefore weakly interacting, Si/Al bonds. Also the coupling between the boundaries and the grain interior appears weaker in Si/Al than in Si. As shown by Figures 3B and 3A, the value of the coordination of the boundary atoms is approximately one in Si/Al and two in Si. This mild action is also supported by the values of the stress tensor which is negligibly low both in Si and in Si/Al (details on this last point have been omitted for the sake of conciseness). Second, the grain relaxation shows the tendency towards an increase of the Al/Al coordination while the Si/Al one remains almost constant (the Al/Al and Al/Si coordinations are shown in Figure 3B. The high value of the Al/Al coordination is due to the large radius used for the evaluation of this parameter, i.e. 4 at the beginning of the relaxation. This trend is independent on the Hamiltonian, though the values of the coordination obviously depend on it. Furthermore the value of the height Z is nearly constant at all sizes (this curve is marked by the arrows in Fig. 3B). This is in itself suggestive that the average height of the z coordinates of the aluminum atoms is maintained (this result holds almost identically for both DFT and SE. The SE values have been therefore omitted for the sake of clarity in the figure) and the view of the relaxed lattices shows this to be the case. These properties indicate the formation of flat, two-dimensional aluminum clusters on the grain surface. Similar flat structures are also reported for films of monolayer thickness deposited onto bulk samples [33].

The properties of the electronic charge are presented in Figures 6 and 7, which show the characteristic energies and DOS, respectively, of Si/Al. In these figures a comparison between the compound and the pure systems is also made. The plots in Figure 6 indicate an upwards shift of the entire eigenvalue spectrum which appears as a perceptible increase of E_b and E_f (for E_f only the DFT evaluation is reported as the SE evaluation shows a similar scaling with the aluminum content). This increase is equal for the two energies and has a similar size-dependence. The effect is obviously attributable to the presence of the aluminum atoms. Furthermore the value one of the coordination between silicon and aluminum (Fig. 3B)

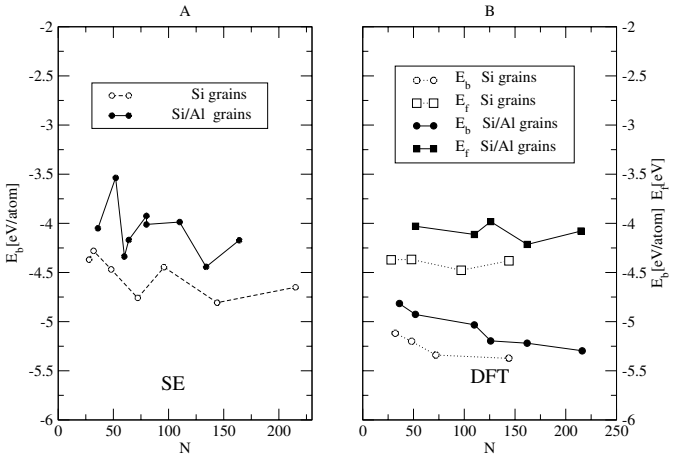

Fig. 6. The functional E_b on the grain size in Si and Si/Al A: SE calculations. B: DFT calculations. In this last case also the Fermi energy E_f is reported.

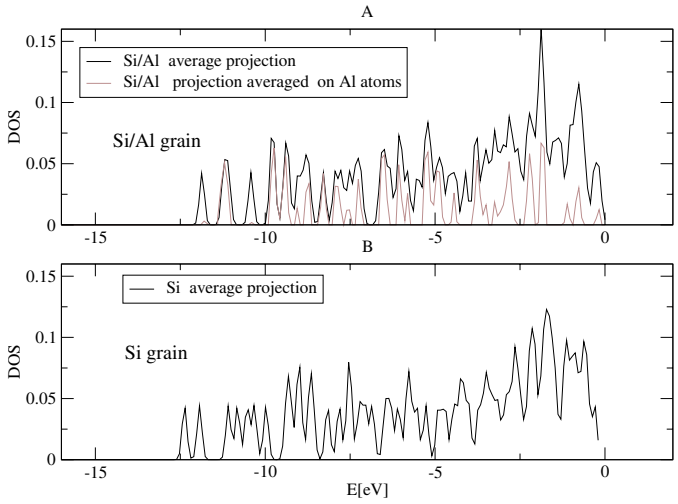

Fig. 7. The DOS plot for N in the range 32. A:Si/Al grain. The figure shows the projection onto the average Si atom and the boundary Al atom A:Si grain. Projection onto the average Si atom.

indicates a short range interaction between Si and Al. Accordingly, the energy increase is spatially located between the aluminum atoms and the silicon atom coordinated with them while the E_f value in the grain interior is equal to the one in the pure Si grains. In electronic devices of standard size the height of the Schottky barrier is evaluated by the upward band bending at the silicon/metal interface. The discussion above indicates that in the case of grains the eigenvalue spectrum localized on the grain boundaries can be obtained from the difference between the energies E_f in Si and in Si/Al grains. The data in the figure indicate that a Schottky barrier exists, is mildly dependent on N and its value falls in the range 0.5 eV. The comparison between the DOS in Si and in Si/Al grains (Fig. 7) shows that in Si/Al the quasi-particle character of the DOS at small N is further enhanced by the splitting into more distinguishably separate peaks. The DOS of the aluminum atoms, also reported in the figure, indicates that the physical origin of this shape has to be sought in the Al charges on the grain boundaries and in the limited exchange and hybridization of these charges with the silicon underneath. Conceptually similar results are presented in [27] where the presence of aluminum atoms on the silicon surface is studied using LDA. These calculations show that linewidths in the DOS plots at 2 eV below E_f arise from the aluminum charge and from its interaction with the silicon atoms. A prerequisite for a quantized conductance G is a DOS shape formed by separate linewidths leading to an expression $G = \sum_j G_o \delta(E - E_j)$. The plots in Figure 7 indicate that this asymptote is best approached by the small Si/Al grains than in the other cases.

As a final note, some comments on the accuracy of the two Hamiltonians are in order. An enlightening perspective into this problem is given by [35]. In this study a detailed comparison between different simulation methods applied to silicon clusters with size N in the range 10 has been performed. The interesting conclusion of this study is that differences in the geometric structure and electronic properties are unavoidable and arise from the multireference structure of silicon clusters. On the other side, a more detailed comparison with literature results is difficult because theories and experiment refer to structures of a different size and/or of a different shape than the ones considered in this study. The few data available have been reported above and their analysis indicates that these results are consistent with the ones in the present study. Furthermore the qualitative agreement between the predictions of the SE and DFT Hamiltonians is evident. Quantitative disagreements are (i) the tendency towards the formation of compressed structures with shorter bonds in SE calculations (Figs. 2, 3) and (ii) the overbinding in DFT (Figs. 4, 6). A detailed comparison of the SIESTA method applied to bulk silicon with calculations based on plane waves expansion [19] indicates that this last failure arises from the exchange-correlation functional and from the limited basis set. Tests on grains with N in the range 40–80, carried out in the course of this study, showed that the use of GGC, instead of LDA, increases E_b of approximately 0.5 eV so that the SE and DFT values are almost coinciding. This, however, delays the convergence of the optimization procedure and considerably increases the computer time. A more limited E_b increase, in the range 0.1 eV, arises from the replacement of single-ζ with double-ζ basis set while the effects of the polarized functions are almost inappreciable. The inadequacy of the SE parametrization to describe the bondlength distribution existing within grains accounts for the shorter lengths obtained from SE (Figs. 2 and 3). No attempt has been made to improve the built-in AM1 parametrization as an effort in this direction is outside the purpose of this work.

5 Conclusions

In conclusion, in this study the structural and electronic properties of nanocrystalline grains have been described

and compared with the ones arising from the presence of an aluminum layer. The electronic configuration of the grains is perceptibly altered by the metallic film and its binding strength is generally reduced. The eigenvalue spectrum shows the formation of a Schottky barrier and the DOS plots shows localization effects. Both features open interesting perspectives for devices applications.

References

1. N.D. Lang, Phys. Rev. B. **52**, 5335 (1995)
2. C.K. Yang, J. Zhao, J.P. Lu, Phys. Rev. B. **66**, 41403R (2002)
3. J.J. Palacios, A.J. Peres-Jimenez, E. Louis, E. SanFabian, J.A. Verges, Phys. Rev. Lett. **90**, 106801 (2003)
4. J. Taylor, H. Guo, Jan Wang, Phys. Rev. B **63**, 245407 (2001)
5. A.M. Mazzone, Material Sci. Eng. B **110**, 152 (2004)
6. A.M. Mazzone, Physica E **27**, 204 (2005)
7. P. Melinon, P. Kegelian, B. Prevel, A. Perez, G. Guiraud, J. LeBrusq, J. Lerne', M. Pellarin, M.J. Broyer, J. Chem. Phys. **107**, 23, 10278 (1997)
8. F. Zignani, A. Desalvo, E. Centurioni, D. Iencinella, R. Rizzoli, C. Summonte, A. Migliori, Thin Solid Films **451**, 350 (2004)
9. H. Hofmeister, J. Dutta, H. Hofman, Phys. Rev. B **54**, 2856 (1996)
10. I. Vasiliev, S. Ögut, J.R. Chelikowski, Phys. Rev. Lett. **86**, 1813 (2001)
11. D.K. Yu, R.Q. Zhang, S.Y. Lee, Phys. Rev. B **65**, 245417 (2002)
12. A. Puzder, A.J. Williamson, F.A. Reboredo, G. Galli, Phys. Rev. Lett. **91**, 157405 (2003)
13. H.Ch. Weissker, J. Forthmüller, F. Bechstedt, Phys. Rev. B **69**, 115310 (2004)
14. G. Belomoin, E. Rogozhina, J. Therrien, P.V. Braun, L. Abuhassan, M.H. Nayfeh, L. Wagner, L. Mitas, Phys. Rev. B **65**, 193406 (2002)
15. M. Haruta, T. Kobayashi, H. Samo, T. Yamada, Chem. Lett. **2**, 405 (1987)
16. MOPAC Quantum Chemistry Program Exchange: Program Number 571, Method, options and tests on MOPAC are described by M.S.J. Dewar, W.J. Thiel, J. Am. Chem. Soc. **99**, 4899 (1987); J.P. Stewart, J. Comput. Chem. **10**, 209 (1989), Other information can be found at the web site `www.indiana.edu`
17. J. Shoemaker, L.W. Burggraf, M.S. Gordon, J. Chem. Phys. **112**, 2994 (2000)
18. A.M. Mazzone, Comput. Mater. Sci. **935** (2002)
19. J.M. Soler, E. Artacho, J.D. Gale, A. Garcia, J. Junquera, P. Ordejon, D. Sanchez-Portal, J. Phys. Condens. Matter **14**, 2745 (2002)
20. K. Raghavachari, V. Logovinsky, Phys. Rev. Lett. **55**, 2853 (1985)
21. K. Raghavachari, C.M. Rohlfing, J. Chem. Phys. **89**, 2219 (1988)
22. Z.Y. Lu, C.Z. Wang, K.M. Ho, Phys. Rev. B **61**, 2329 (2000)
23. A.A. Shvartsburg, M.F. Jarrold, B. Liu, Z.-Y. Lu, C.Z. Wang, K.M. Ho, Phys. Rev. Lett. **81**, 4616 (1998)
24. I. Rata, A.A. Shvartsburg, M. Hiroi, T. Fraunenheim, K.W.M. Siu, K.J. Jackson, Phys. Rev. Lett. **546**, 85 (2000)
25. B.K. Panda, S. Mukherjee, S.N. Behera, Phys. Rev. B **63**, 45404 (2001)
26. X.G. Gong, Phys. Rev. B. **52**, 14677 (1995)
27. J.R. Chelikowsky, Phys. Rev. B **16**, 3618 (1977)
28. I.K. Robinson, P.A. Bennet, F.J. Himpsel, Phys. Rev. Lett. **88**, 96104 (2002)
29. H.I. Zhang, M. Schluter, J. Vac. Sci. Technol. **15**, 1384 (1978)
30. J.E. Northrup, Phys. Rev. Lett. **53**, 683 (1984)
31. M. Nishida, Phys. Stat. Sol. (b) **95**, 263 (1979)
32. B.N. Dev, S.M. Mohapatra, K.C. Mishra, W.M. Gibson, T.P. Das, Phys. Rev. B **36**, 2666 (1987)
33. V.G. Zavodinsky, I.A. Kyanov, Computational Material Science **11**, 138 (1998)
34. D. Porezag, Th. Frauenheim, Th. Köhler, G. Seifert, R. Kaschner, Phys. Rev. B **51**, 12947 (1995)
35. A. Tekin, B. Hartke, Phys. Chem. Chem. Phys. **6**, 503 (2004)